Liquid Crystals
Publication details, including instructions for authors and subscription information:
http://www.informaworld.com/smpp/title~content=t713926090

Amplitude and phase fluctuation modes in the smectic C_α^* phase of an antiferroelectric compound

M. B. Pandey[a]; R. Dhar[b]; R. Dabrowski[c]
[a] Physics Department, University of Allahabad, Allahabad-211 002, India [b] Physics Department, Ewing Christian College, Allahabad-211 003, India [c] Institute of Chemistry, Military University of Technology, 00-908, Warsaw, Poland

To cite this Article Pandey, M. B. , Dhar, R. and Dabrowski, R.(2008) 'Amplitude and phase fluctuation modes in the smectic C_α^* phase of an antiferroelectric compound', Liquid Crystals, 35: 7, 777 — 787
To link to this Article: DOI: 10.1080/02678290802175749
URL: http://dx.doi.org/10.1080/02678290802175749

Liquid Crystals,
Vol. 35, No. 7, July 2008, 777–787

Taylor & Francis
Taylor & Francis Group

Amplitude and phase fluctuation modes in the smectic C_α* phase of an antiferroelectric compound

M. B. Pandey[a]*, R. Dhar[b] and R. Dabrowski[c]

[a]*Physics Department, University of Allahabad, Allahabad-211 002, India;* [b]*Physics Department, Ewing Christian College, Allahabad-211 003, India;* [c]*Institute of Chemistry, Military University of Technology, 00-908, Warsaw, Poland*

(Received 23 November 2007; final form 1 May 2008)

Dielectric measurements have been carried out on the chiral smectic C_α (SmC_α*) phase of a MHPOBC analogous compound. Two relaxation modes have been observed in this phase for planar orientation of the molecules. One process has been observed at frequency lower than that of the soft mode of the chiral smectic A (SmA*) phase. This relaxation process is connected with the helicity of the SmC_α* phase. In the high-frequency region, another relaxation process has been observed in the SmC_α* phase for which bias field dependence is similar to that of the soft mode at the SmA*–SmC* phase transition. The experimental observations are in agreement with a recently proposed dielectric theory for the SmC_α* phase and theoretical dielectric results obtained by numerical simulations. Thus, we report here experimental verification of two theoretically predicted dielectric modes in the SmC_α* phase.

Keywords: dielectric relaxation; soft mode; chiral phases; SmC_α* phase; bias field dependence

1. Introduction

There has been a considerable interest in understanding the structure of novel phases possessed by antiferroelectric liquid crystals (AFLCs). The discovery of subphases was associated with the discovery of an antiferroelectric phase in MHPOBC (*1–3*). One variant of the chiral smectic C (SmC*) phase, the chiral smectic C_α (SmC_α*) phase, has been shown to exhibit an incommensurate nanoscale helical pitch (*4*). Different experimental techniques such as resonant X-ray scattering (*4*), dielectric spectroscopy (*5–8*), optical rotation (*9*), light scattering on freely suspended films (*10*), nonlinear dielectric spectroscopy (*11, 12*) and helical pitch measurements (*13*) have been used to characterise the structure of the SmC_α* phase. X-ray diffraction data show that the SmC_α* phase is a tilted smectic. On the basis of resonant X-ray studies, Mach *et al.* (*4*) have shown that the SmC_α* phase has incommensurate structure with a modulation period between five and eight smectic layers. Recently it has been reported that modulation period of SmC_α* phase varies less than four smectic layers (*14*). In spite of the tilt, the phase is uniaxial and it is not easy to distinguish the SmC_α* phase from a chiral smectic A (SmA*) phase on the basis of optical studies (*2, 3, 13*).

Dielectric spectroscopic investigations have become an important tool to study such systems because of their capability of providing information about the individual molecular and collective modes involved in these phases. In the dielectric spectrum of the SmC_α* phase most often only one collective relaxation process is observed that exists in the high kHz region (*5–8*). The origin of this mode is assigned to tilt fluctuation of molecules, i.e. a soft mode. In some materials, a collective mode in the low kHz region has also been reported and its origin has been assigned to a Goldstone mode (*7, 8*). However, from electro-optical measurements, Bourny *et al.* have reported two relaxation modes in the SmC_α* phase of MHPOCBC and their origins are assigned to be soft and ferroelectric modes, respectively (*15*). Conradi *et al.* have theoretically studied freely suspended thin films of the SmC_α* phase in an external electric field within the 'clock model'. They have predicted the occurrence of *n* amplitudes and *n* phase fluctuation modes for *n* smectic layers in one helical pitch of the SmC_α* phase (*10*). They have calculated relaxation rates in the kHz range for phase fluctuation modes and several MHz for amplitude fluctuation modes. Vaupotic *et al.* have proposed a theoretical model that describes the dielectric properties of SmC_α* and other chiral phases in bulk on the basis of a discrete phenomenological model ('clock model') (*16*). They have predicted two dielectric relaxation processes, i.e. amplitude and phase fluctuation modes in the SmC_α* phase. They have calculated that relaxation frequency and the inverse of dielectric strength of the amplitude mode should increase upon cooling in the SmC_α* phase; however, the relaxation frequency of phase

*Corresponding author. Email: mbpandey@gmail.com

ISSN 0267-8292 print/ISSN 1366-5855 online

DOI: 10.1080/02678290802175749
http://www.informaworld.com

modes should be temperature independent. Similar features have also been reported by Douali *et al.* by a numerical simulation method for different values of azimuthal angle difference (α) between two successive smectic layers (*17*). Douali *et al.* have also carried out dielectric and azimuthal angle difference (α) measurements on the SmC_α* phase and proposed a correlation between dielectric and optical parameters. They have shown that a Goldstone mode will be dominant for low values of $\alpha < 25^\circ$. In this case, a soft mode can not be observed without application of a bias electric field. As the value of α increases, the dielectric strength of the Goldstone mode decreases and the soft mode contribution is predominant in the vicinity of the SmA*–SmC_α* transition. However, they were unable to observe these two dielectric modes simultaneously at a common temperature as predicted by theory and numerical simulation results (*16, 17*).

In this paper, we report the dielectric characterisation of the SmC_α* phase of a room temperature antiferroelectric liquid crystal, (*S*)-4′-octyloxybiphenyl-4-carboxylic acid 3-chloro-4-(1-methylheptyloxycarbonyl) phenyl ester (Cl-MHPOBC) (*18*). The aim of the present work was to obtain experimental verification of the theoretically predicted two dielectric relaxation modes in the SmC_α* phase and their temperature and bias field dependence.

2. Experimental

Different mesophase transition temperatures were determined by using differential scanning calorimetry (DSC, Setaram model DSC 141). Dielectric measurements were carried out using a cell of thickness 5 μm, the surfaces of which were chemically treated to ensure planar orientation. The dielectric data of capacitance (C) and conductance (G) in parallel mode were acquired with the help of impedance/gain-phase analyser (Solartron model SI-1260) coupled with a Solartron dielectric interface (model 1296). A measuring ac electric field of 0.1 V_{rms} was applied across the sample in the direction parallel to the smectic layers. In order to study the bias electric field dependence of the dielectric permittivity and relaxation frequency, a dc voltage of 0 to 40 V was superimposed on the measuring ac field using a SI-1260 bridge. The cell was also used for texture studies. The temperature of the sample was controlled with the help of a hot stage (Instec model HS-1) with an accuracy of $\pm 0.1^\circ$C. The local temperature near the sample was determined by measuring the thermo emf of a copper–constantan thermocouple with the help of a six and half digit multimeter with an accuracy of $\pm 0.1^\circ$C. Other details of experimental techniques are discussed elsewhere (*19*).

To analyse the measured data, the dielectric spectra were fitted with the help of the Havriliak and Negami (HN) equation (*18–20*):

$$\varepsilon^* = \varepsilon' - j\varepsilon'' = \varepsilon'(\infty) + \sum_i \frac{\Delta\varepsilon_i}{\left[1 + (j\omega\tau_i)^{(1-h_i)}\right]^{\beta_i}} + \frac{A}{\omega^n} + \frac{\sigma_{ion}}{j\varepsilon_0\omega} - jB\omega^m, \quad (1)$$

where ε' (∞) is the high-frequency limiting value of the relative permittivity and $\Delta\varepsilon_i$, τ_i and h_i are the dielectric strength, the relaxation time (inverse of angular relaxation frequency) and the symmetric distribution parameter ($0 \leqslant h_i \leqslant 1$) of i^{th} mode, respectively. β_i is an asymmetric distribution parameter. The third and fourth terms in equation (1) are added due to the presence of electrode polarisation capacitance and ionic conductance at low frequencies, where A and n are fitting constants (*21, 22*). σ_{ion} is the ionic conductance and ε_0 ($=8.85\,pF\,m^{-1}$) is the permittivity of free space. The fifth imaginary term $B\omega^m$ (*22, 23*) is included in equation (1) to partially account for the high-frequency ITO effect, where B and m are constants since correction terms are small.

An example of mode analysis at 97.0°C using equation (1) from low- and high-frequency artefacts is shown in Figure 1. The uncertainty in determination of the relaxation frequency (f_R) and dielectric strength ($\Delta\varepsilon$) is less than $\pm 3\%$ for both modes. Uncertainties in the determination of the distribution parameters (h) increases up to $\pm 10\%$ due to weak strength, overlapping of two modes and other artefacts, as discussed above. The value of β_i in equation (1) has been found to be unity at all temperatures. However, these uncertainties are small in the SmA* and SmC* phases as compared to SmC_α* phase.

3. Results and discussion

DSC and optical texture studies

DSC thermograms revealing transitions between the different chiral smectic C phases in the investigated compound are shown in Figure 2. DSC peaks corresponding to SmC_A*–SmC_γ*, SmC_γ*–SmC* and SmC_α*–SmA* transitions have been clearly observed, whereas the SmC*–SmC_α* transition appears as a shoulder, although it is clear enough to represent the transition.

The optical textures of the SmA*, SmC_α* and SmC* phases of the compound are shown in Figure 3

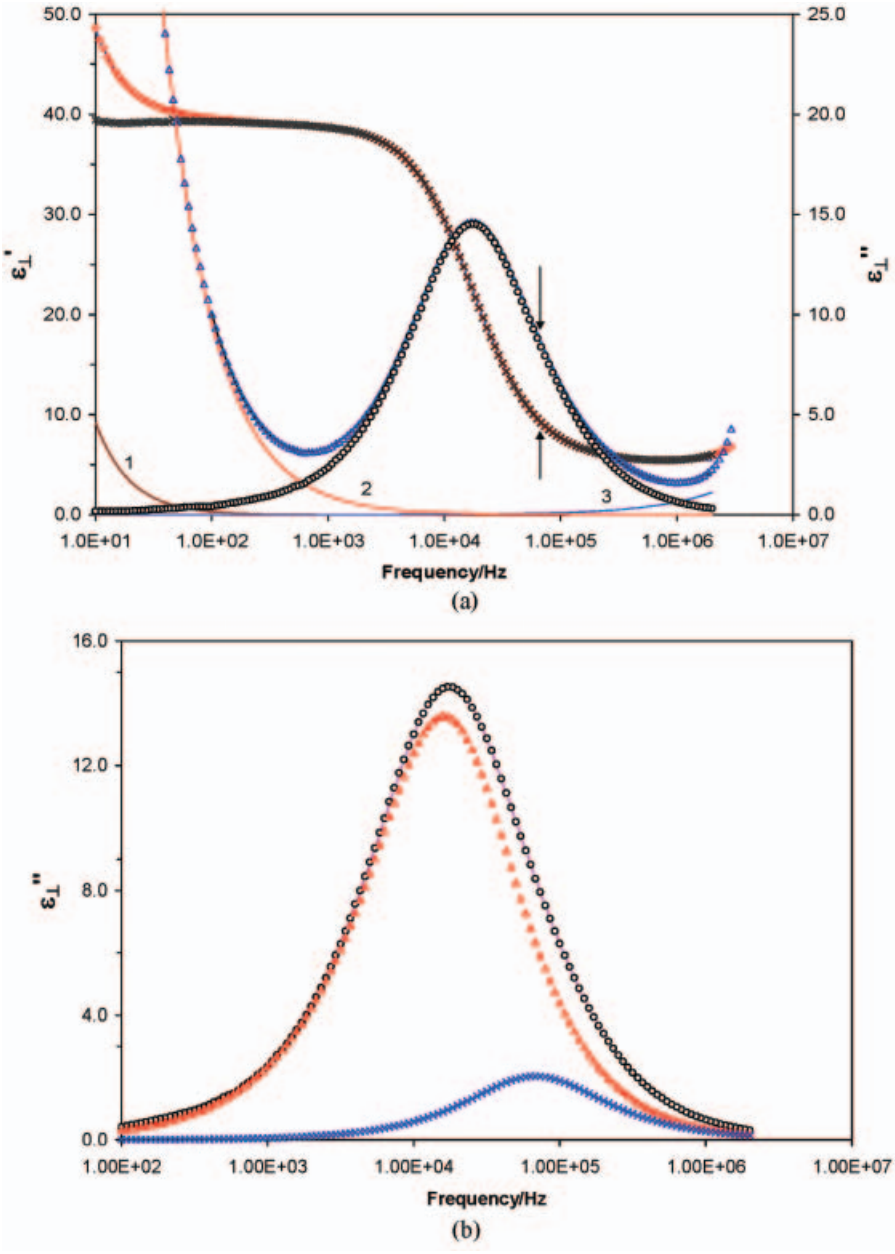

Figure 1. (a) An example of mode separation by simulation of measured data of ε' (open squares) and ε'' (open triangles) in the SmC_α* phase at 97.0°C using equation (1). Solid lines with experimental data are fitted curve. Low-frequency corrections (LFC) due to the electrode polarization and ionic conductance in ε' and ε'' data are shown by curves 1 and 2, respectively. High-frequency corrections (HFC) in ε'' data due to the ITO effect are shown by curve 3. Corrected data of ε' and ε'' after subtracting LFC and HFC from the measured data are shown by open crosses and circles, respectively. Vertical arrows mark a weak relaxation mode on the high-frequency side, which has been masked due to HFC and the presence of another stronger mode on the low-frequency side. (b) The corrected ε'' data (open circles) of (a) have been fitted with two Cole–Cole mechanisms (solid lines). Two relaxation processes (loss curves) at low and high frequencies are separated mathematically and shown by open triangles and crosses, respectively.

for a planar-aligned sample of thickness 5 µm upon cooling from the isotropic phase. As can be seen from Figure 3, complete homogeneous alignment was not possible in this material and a few defect lines are observed in all the phases. The SmA*–SmC_α* phase transition did not produce any drastic change in the texture and only a slight change in the colour of the texture has been observed. The transition to SmC* phase, on the other hand, has been easily spotted due to appearance of unwinding of helix lines (see Figure 3(c)). The large pitch of the SmC* phase in comparison to the SmC_α* phase led to the

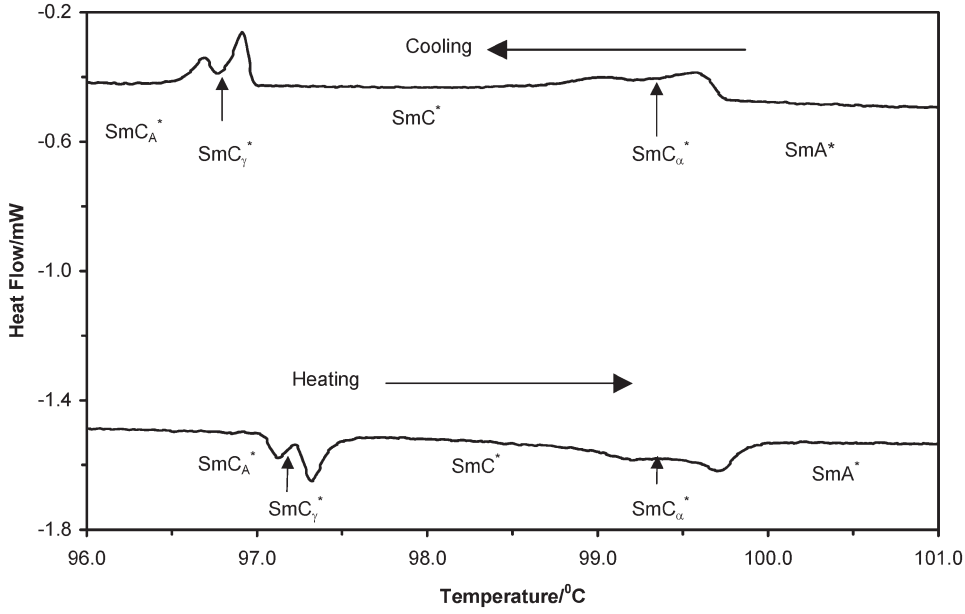

Figure 2. DSC thermograms of Cl-MHPOBC representing transitions between SmA*, SmC_α*, SmC*, SmC_γ* and SmC_A* phases, in the heating and cooling cycles at a scanning rate of $0.2^\circ C\,min^{-1}$.

appearance of these equally spaced dechiralisation lines perpendicular to the defect lines (*13*). Transition temperatures obtained from DSC and optical texture studies/dielectric parameters (discussed in forthcoming paragraphs) are slightly different. Such differences have also been reported earlier and are not surprising because appearance of these phases and transition temperatures sensitively depends on the sample history, surface condition and also on the thickness of the sample (*18*). Mode of temperature change during the different experiment may also be responsible for the observed difference in transition temperatures.

Dielectric studies

A detailed discussion of the relaxation processes of chiral SmC sub-phases and the SmC_A* phase has been published elsewhere (*24, 25*). We, therefore, concentrate here only on the relaxation modes of the SmC_α* phase and its two adjacent phases (SmA* and SmC*). Figure 4 shows various absorption curves at different temperatures for the SmA* and SmC_α* phases. In the SmA* phase, the dielectric absorption spectrum contains only one peak, which increases in strength and its corresponding relaxation frequency decreases with decrease in temperature. At the onset of the SmC_α* phase (97.6°C), another mode with high dielectric strength appears in the dielectric spectrum on the low-frequency side. This mode is coupled with another weak mode towards the high-frequency side. This is evidenced by Figure 4, where the right hand (high frequency) side of the dielectric absorption curve remains unchanged but expands towards left hand (low frequency) side upon cooling in the SmC_α* phase. The high-frequency mode could not be observed clearly due to its weak nature in comparison to the low-frequency mode, the presence of high-requency effects and cell relaxation above 4 MHz (see Figure 4).

However, we were able to obtain the dielectric parameters related with these two modes by a fitting process. Initially, low- and high-frequency effects are subtracted from the experimental data. The corrected data have then been fitted with one HN mechanism and two Cole–Cole mechanisms separately. The deviation (residual plot) of the fitted curves with corrected data is shown in Figure 5. In the case of fitting with one HN mechanism, a weak relaxation process is clearly visible at 100 kHz in the residual plot. The value of the residual plot is found to be negative at high frequencies. When the corrected experimental data have been fitted with two Cole–Cole mechanisms, excellent fitting has been found, as shown in Figure 5(b). The residual plot has been found to be approximately zero and linear at high frequencies. In addition, the value of relaxation frequencies also coincide with those obtained from fitted and residual plots of one HN mechanism. Therefore, all experimental curves are fitted with two Cole–Cole mechanisms and results are presented here.

The dielectric strength ($\Delta\varepsilon$) and relaxation frequency (f_R) of the modes present in the SmA*,

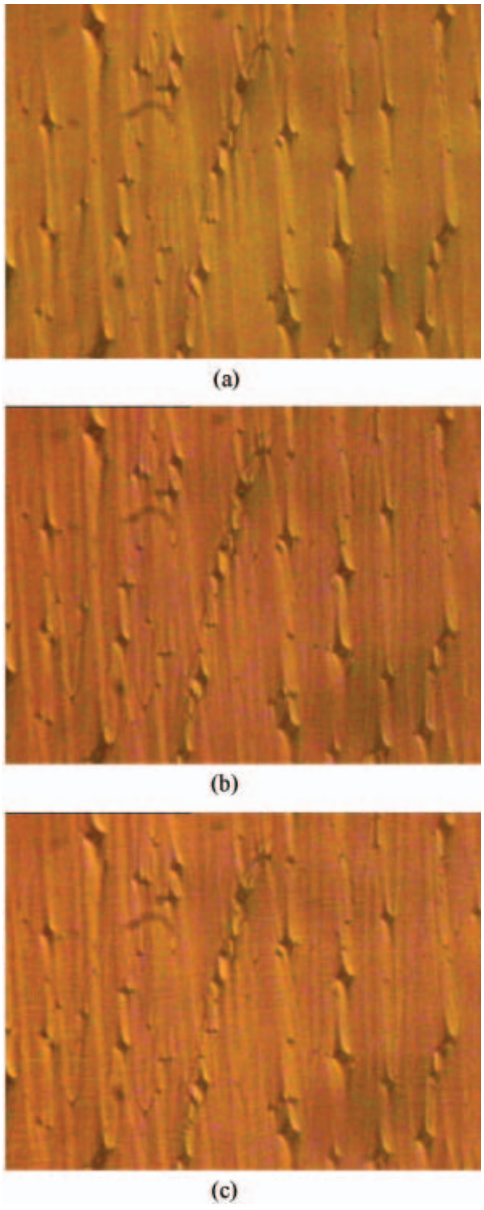

Figure 3. Optical textures (100×) of different phases of Cl-MHPOBC under crossed polariser conditions for planar aligned sample: (a) SmA* phase at 99.5°C; (b) SmC_α* phase at 97.2°C; (c) SmC* phase at 96.1°C in the cooling cycle.

SmC_α* and SmC* phases have been obtained by fitting process and are shown in Figures 6a and 6b, respectively. In the SmA* phase, the relaxation mode (M_1) possesses high frequency and low dielectric strength. On cooling the sample, relaxation frequency and inverse of dielectric strength (Figure 6(c)) of mode M_1 decreases linearly with decrease in temperature, as predicted by theoretical models (*3, 26*). The distribution parameter (h) of M_1 has been found to be approximately zero in the cooling cycle. In the heating cycle, the value of h is found to be ~0.1. On the basis of above observations, we assign the M_1 process to a soft mode linked with amplitude fluctuations of the tilt angle θ (*2, 3, 26*).

Tables 1 and 2 show the slopes of the curves of $\Delta\varepsilon^{-1}(T)$ and $f_R(T)$ in the heating and cooling cycles. The slopes of $f_R(T)$ in the heating and cooling cycles have been found to be slightly different for M_1. The small difference in slopes during two cycles are attributed to different sample history in the heating (transition from tilted SmC_α* to orthogonal SmA*) and cooling (transition from isotropic liquid to orthogonal SmA*) cycles.

In the SmC_α* phase, two relaxation modes (M_2 and M_3) have been observed, as shown in Figure 6(b). The relaxation frequencies of M_2 and M_3 decrease with a decrease in temperature. The magnitude of variation, i.e. slope, of M_3 is large as compared to that of M_2. Discontinuities have been observed in the plots of dielectric strength and inverse dielectric strength at the SmA*–SmC_α* transition (Figure 6). Dielectric strengths of M_2 and M_3 increase with decrease in temperature throughout the SmC_α* phase. The distribution parameter of M_2 increases continuously with decrease in temperature between 0.05 and 0.20, whereas the distribution parameter corresponding to M_3 has been found to be approximately zero throughout the SmC_α* phase. The values of various dielectric parameters ($\Delta\varepsilon$, f_R and h) corresponding to M_2 and M_3 are found to be approximately same in both heating and cooling cycles.

In the SmC* phase (in the cooling cycle), relaxation frequency of M_2 becomes invariant (~5 kHz) with temperature and possesses high dielectric strength (Figure 6). The distribution parameter has also been found to be constant (~0.20). On the basis of its typical behaviour this relaxation process has been assigned to the Goldstone mode related with the phase fluctuations of the tilt angle (θ). In the case of M_3, no pronounced change has been observed in its relaxation frequency but inverse dielectric strength increases with decrease in temperature in the SmC* phase (see Figure 6). The distribution parameter of this mode is found to be zero throughout the SmC* phase. This mode is similar to typical soft mode behaviour across the SmA*–SmC* phase transition in ferroelectric liquid crystal materials.

To understand the origin of relaxation processes in the SmC_α* phase, we have carried out dielectric measurements with a bias electric field. Figure 7 shows dielectric absorption spectra at 97.3°C (below the SmA*–SmC_α* transition) and 97.0°C (close to the SmC_α*–SmC* transition) with bias electric field varying from 0 to 60 kV cm^{-1}. Relaxation frequencies of modes M_2 and M_3 remain invariant up to 12 kV cm^{-1}. At higher electric fields, the relaxation

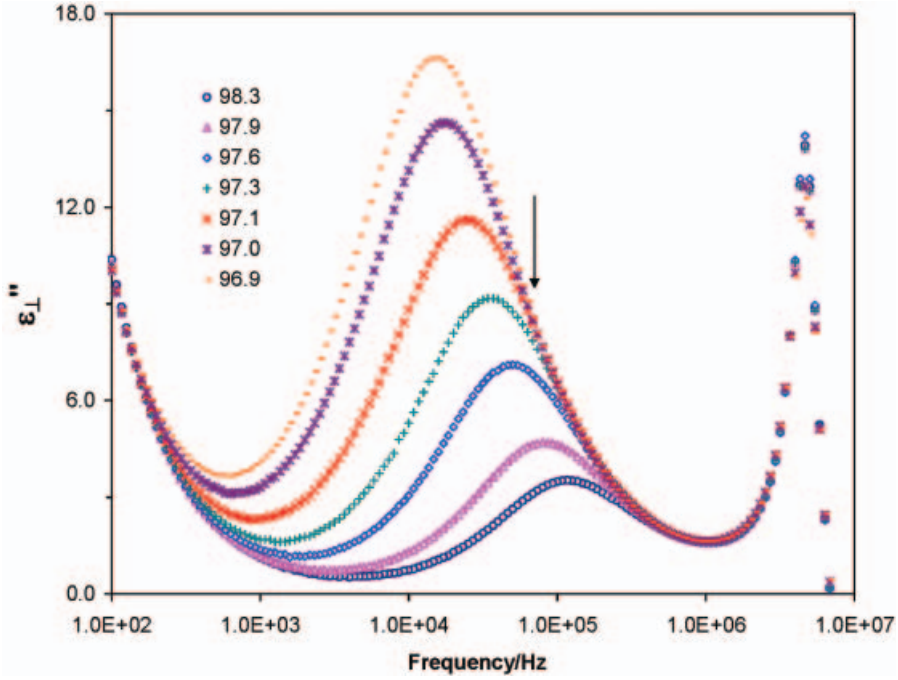

Figure 4. Dielectric absorption spectra at various temperatures in the SmA* (98.3 and 97.9°C) and SmC_α* (97.6, 97.3, 97.1, 97.0 and 96.9°C) phases of Cl-MHPOBC. The downward vertical arrow marks a weak relaxation mode at high frequency in the SmC_α* phase, which is not clearly visible due to presence of a stronger mode at low frequency and HFC.

process M_2 shifts towards the high-frequency side and its dielectric strength is strongly reduced. The combined effect of shifting the M_2 process to the high-frequency range, the weak nature of the M_3 mode and the dominance of the HFC term above 1 MHz make it difficult to obtain dielectric parameters of M_2 and M_3 within reasonable uncertainty limits after application of a bias electric field. The M_2 process was completely suppressed above a critical field of 36 kV cm^{-1}. This result confirms that the M_2 process is connected with the helicity of the phase.

The temperature dependence of the relaxation frequency and dielectric strength in the SmA*, SmC_α* and SmC* phases at 40 and 60 kV cm^{-1} bias electric fields are shown in Figures 8 and 9, respectively. With a bias electric field (at 40 kV cm^{-1}) the relaxation frequency and dielectric strength exhibit minimum and maximum values near the SmA*–SmC_α* transition. $\Delta\varepsilon^{-1}$ and f_R exhibit a linear temperature dependence above and below the SmA*–SmC_α* transition. This behaviour is characteristic of a soft mode, usually evidenced with measurements under bias electric field in conventional ferroelectric liquid crystals. Hence, the relaxation process observed under bias electric field could be attributed to the soft mode below the SmA*–SmC_α* transition. The slope ratios of the straight lines (see Table 3) fitted to the experimental data ($\Delta\varepsilon^{-1}$) below and above the SmA*–SmC_α* transition are found to be close to the theoretical value (−2.0) predicted for a soft mode by mean field approximations (*26*). However, in the case of f_R, the slope ratios are found to be far from theoretical values. It is important to mention here that soft mode frequency should be bias field independent. We have found similar behaviour in the SmA* phase; where relaxation frequency (far from transition region) does not change appreciably due to application of bias electric field. However, in the tilted smectic (SmC_α* and SmC*) phases, the relaxation frequency changes drastically due to application of a bias electric field (see Figure 8).

At the onset of SmC_α* phase, two relaxation modes have been observed at 100 kHz and 32 kHz, respectively (see Figure 6). Because of high dielectric strength and distribution parameters, the M_2 process may be considered due to the helicity of the SmC_α* phase. Experiments with a bias electric field also support this logic. Hence, the origin of this mode is stipulated as being due to phase fluctuations of the tilt of molecules. The dielectric strength of M_3 without electric field increases in the SmC_α* phase upon cooling and this shows opposite trend as compared to that of SmC* phase. It should also be noted that slope of M_1 (114.3 kHz °C^{-1}) in the SmA* phase is close to the slope of M_3 (101.9 kHz °C^{-1}) in the SmC_α* phase. This result indicates that the SmA*–SmC_α* phase transition should be close to

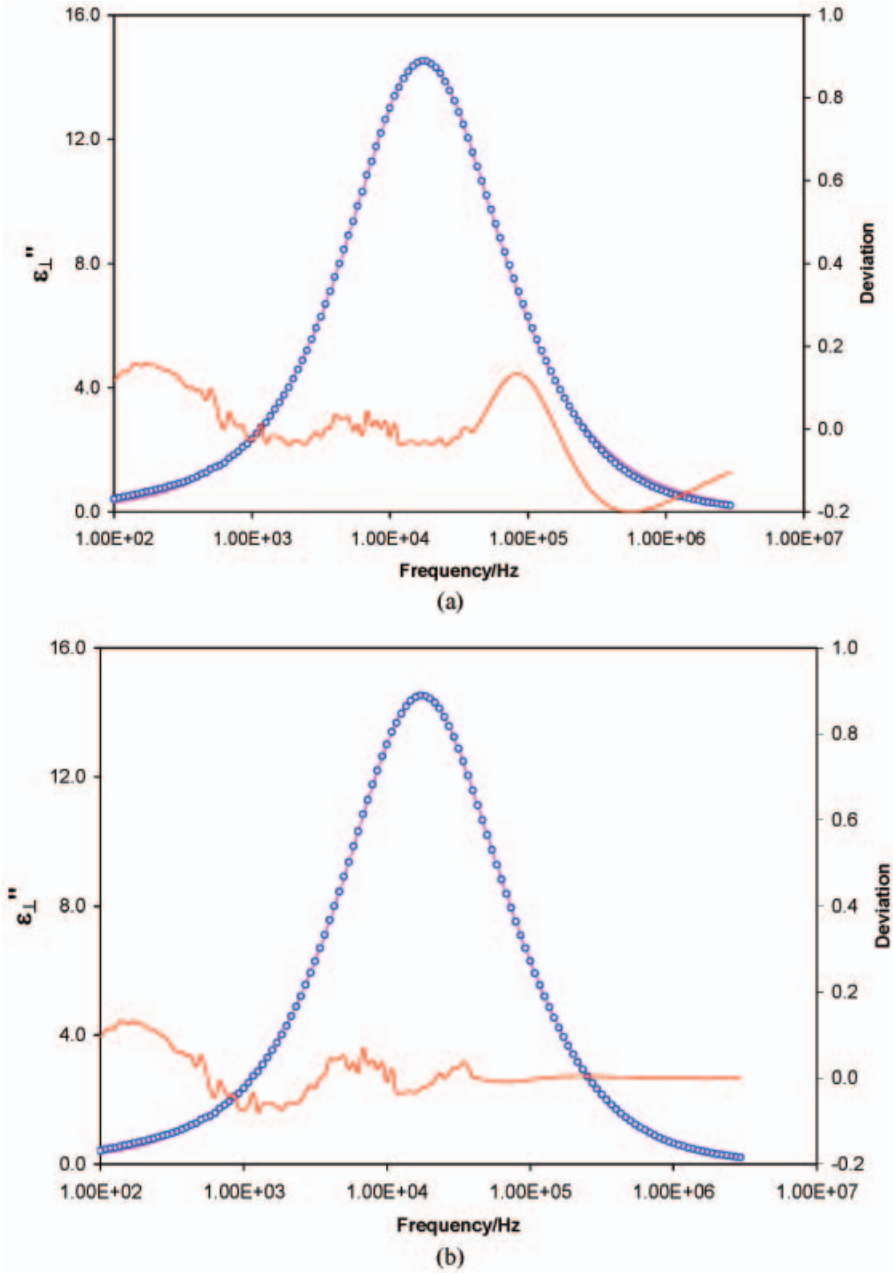

Figure 5. (a) The corrected ε'' data (open circles) of figure 1a fitted with one Havriliak–Negami mechanism (solid lines). The deviation (residual plot) of fitted curve with corrected ε'' data is shown on the secondary y-axis. (b) The corrected ε'' data (open circles) of figure 1a fitted with two Cole–Cole mechanisms (solid lines). The deviation (residual plot) of fitted curve with corrected ε'' data is shown on the secondary y-axis.

the tricritical point, as has been pointed out by Skarabot *et al.* (*27*).

According to theory of Vaupotic *et al.* (*16*) the relaxation frequency of the amplitude mode should increase upon cooling in the SmC_α* phase, whereas the relaxation frequency of the phase mode should be temperature independent. The variation of relaxation frequency of mode M_3 with temperature (without bias electric field) does not seem to follow soft mode behaviour as predicted theoretically (*16, 17*). However, variations of the relaxation frequency and dielectric strength of mode M_2 with temperature in the SmC_α* phase have been found to be similar to those predicted by theory (*16*). The change in the value of relaxation frequency and dielectric strength of M_2 with temperature in the SmC_α* phase may be considered due to the temperature dependence of azimuthal angle difference (α) which decreases with

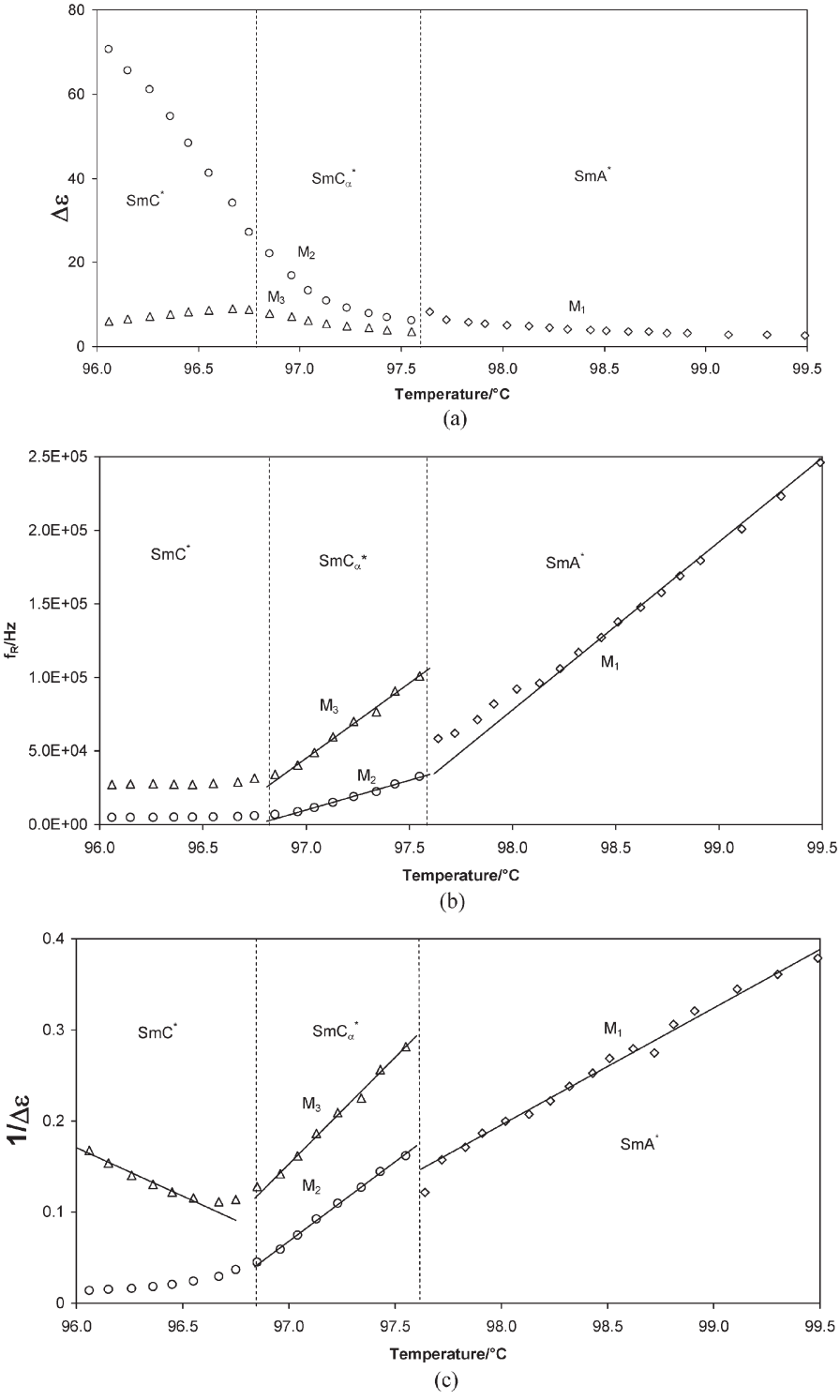

Figure 6. Temperature dependence of (a) dielectric strength ($\Delta\varepsilon$), (b) relaxation frequency (f_R) and (c) inverse of dielectric strength ($1/\Delta\varepsilon$) of various modes of SmA*, SmC$_\alpha$* and SmC* phases of Cl-MHPOBC in cooling cycles. Vertical broken lines show the separation of different phases on the basis of dielectric parameters.

decrease in temperature and vice-versa. This is consistent with the numerical simulation results obtained by Douali *et al.* (*17*). It is worthwhile to mention here that soft mode of the SmC$_\alpha^*$ phase are reported to vary in similar fashion to those of the SmA* phase, i.e. relaxation frequency decreases with decrease in temperature, as observed for other materials (*5–8*, *17, 28*). After application of a bias

Table 1. Slopes of $\Delta\varepsilon^{-1}(T)$ curves (in $^{\circ}C^{-1}$) of modes (M_1, M_2 and M_3) in the SmA*, SmC_α* and SmC* phases of Cl-MHPOBC in heating and cooling cycles.

	SmA*	SmC_α*		SmC*
	M_1	M_2	M_3	M_3
Heating	0.122	0.169	0.225	−0.065
Cooling	0.128	0.174	0.234	−0.081

Table 2. Slopes of $f_R(T)$ curves (in kHz $^{\circ}C^{-1}$) of modes (M_1, M_2 and M_3) in the SmA* and SmC_α* phases of Cl-MHPOBC in heating and cooling cycles.

	SmA*	SmC_α*	
	M_1	M_2	M_3
Heating	125.1	43.2	124.8
Cooling	114.3	40.5	101.9

electric field, f_R and $\Delta\varepsilon^{-1}$ of M_3 increase with decrease in temperature and follow similar behaviour as predicted by theory (see Figures 8 and 9). Hence, the present investigation is in complete conformity with the theoretical predictions of Vaupotic *et al.* and Douali *et al.* across the SmA*–SmC_α* transition (*16, 17*). Douali *et al.* have shown that the soft mode dielectric strength diminishes rapidly to one tenth of its original value closer than ~0.5°C to the SmA*–SmC_α* transition temperature. In the present work, it has been found that soft mode contributions decrease to half their value at ~1.5°C below the transition to the tilted phase with bias electric field. In previous studies (*16, 17*), the authors have presented a theoretical model that describes only a particular phase transition, e.g. SmA*–SmC_α* and SmA*–SmC_A*.

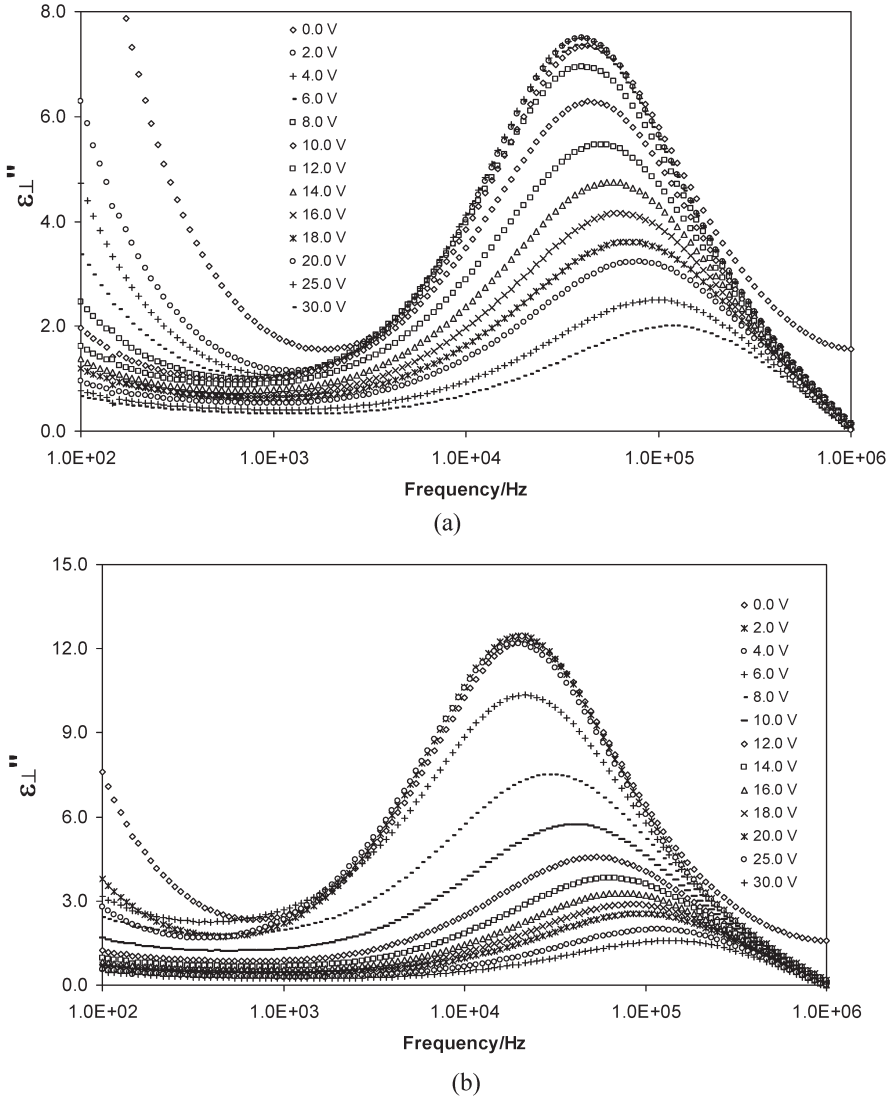

Figure 7. Effect of bias electric field on dielectric absorption spectra (a) in the SmC_α* phase at 97.3°C just below SmA*–SmC_α* transition and (b) at 97.0°C close to SmC_α*–SmC* transition for a sample of thickness of 5 µm.

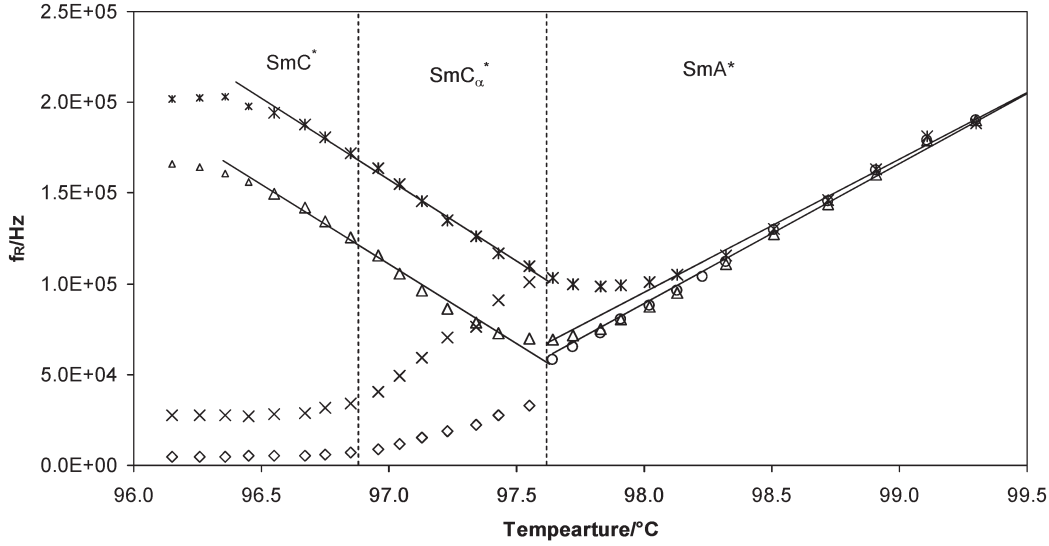

Figure 8. Temperature dependence of the relaxation frequency (f_R) at bias electric fields of 40 kV cm^{-1} (open triangles) and 60 kV cm^{-1} (open doumble) in the SmA*, SmC$_\alpha$* and SmC* phases of Cl-MHPOBC. The relaxation frequencies of modes M_1 (open circles), M_2 (open squares) and M_3 (open crosses) observed without bias electric field are also shown for comparison.

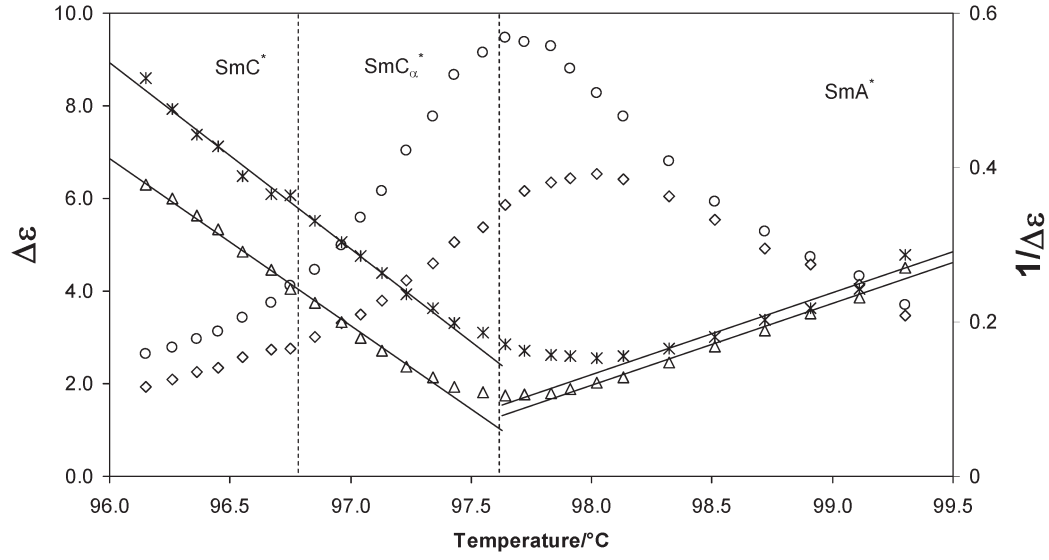

Figure 9. Temperature dependence of the dielectric strength ($\Delta\varepsilon$) at bias electric fields of 40 kV cm^{-1} (open circles) and 60 kV-cm^{-1} (open squares) in the SmA*, SmC$_\alpha$* and SmC* phases of Cl-MHPOBC. Corresponding inverse dielectric strengths ($1/\Delta\varepsilon$) are shown by open triangles and doumbles, respectively.

Table 3. Slopes of $\Delta\varepsilon^{-1}(T)$ and $f_R(T)$ curves of modes observed with a bias voltage (30.0 V and 20.0 V) in SmA* and SmC$_\alpha$* phases of Cl-MHPOBC in the cooling cycle for sample thickness 5 μm.

	SmA* (*a*)		SmC$_\alpha$* (*b*)		*b*/*a*	
	30.0 V	20.0 V	30.0 V	20.0 V	30.0 V	20.0 V
f_R/ kHz °C^{-1}	73.2	76.9	−89.5	−87.49	−1.22	−1.13
$\Delta\varepsilon$/°C^{-1}	0.118	0.106	−0.241	−0.216	−2.04	−2.04

However, one should note that the signs and the values of different parameters of free energy equation taken in in these studies (*16, 17*) are not arbitrary. They depend upon the phase sequence of the compound, the phase transition temperatures and on the values of tilt angle at the different phase transitions (*29*). Hence, there is need of a comprehensive theoretical model that describes the dielectric behaviour of antiferroelectric liquid crystals possessing various chiral smectic phases.

4. Conclusions

Dielectric measurements for a planar-aligned sample in its SmC_α* phase reveal two relaxation processes. The low-frequency mode has been observed between 40 kHz and 8 kHz. It possesses high dielectric strength. The dielectric strength of the low-frequency mode decreases with increase in intensity of electric field and it is suppressed at a critical value of $36\,kV\,cm^{-1}$. Its origin is stipulated as being due to phase fluctuations of the tilt of the molecules. The high-frequency mode possesses small dielectric strength (~4–8) and its frequency varies between 100 kHz and 32 kHz. After application of bias electric field, the relaxation frequency and inverse dielectric strength of the high-frequency mode increases with decrease in temperature throughout the SmC_α* phase. Hence, this mode is considered to be related with amplitude fluctuations of the tilt of the molecules, i.e. a soft mode. The experimental observations support the proposed dielectric theory for the SmC_α* phase on the basis of a 'clock model'.

Acknowledgements

MBP wishes to thank the Department of Science and Technology, Government of India, New Delhi, for financial assistance under a fast-track project for young scientist (SR/FTP/PS-14/2005). The authors sincerely thank to Prof. H. Prakash, Head, Physics Department, and Prof. I. M. L. Das, Physics Department, University of Allahabad, Allahabad, for their support.

References

(1) Chandani A.D.L.; Ouchi Y.; Takezoe H.; Fukuda A.; Terashima K.; Furukawa K.; Kishi A. *Jap. J. Appl. Phys.* **1989**, *28*, L1261–L1264; Chandani A.D.L.; Gorecka E.; Ouchi Y.; Takezoe H.; Fukuda A. *Jap. J. Appl. Phys.* **1989**, *28*, L1265–L1268.
(2) Fukuda A.; Takanishi Y.; Isozaki T.; Ishikawa K.; Takezoe H. *J. Mater. Chem.* **1994**, *4*, 997–1016.
(3) Musevic I.; Blinc R.; Zeks B. *The Physics of Ferroelectric and Antiferroelectric Liquid Crystals*; World Scientific: Singapore, 2000.
(4) Mach P.; Pindak R.; Levelut A.M.; Barois P.; Nguyen H.T.; Huang C.C.; Furenlid L. *Phys. Rev. Lett.* **1998**, *81*, 1015–1018.
(5) Cepic M.; Heppke G.; Hollidt J.M.; Lotzsch D.; Moro D.; Zeks B. *Mol. Cryst. Liq. Cryst.* **1995**, *263*, 207–216.
(6) Merino S.; de la Fuente M.R.; Gonzalez Y.; Perez Jubindo M.A.; Ros B.; Puertolas J.A. *Phys. Rev. E* **1996**, *54*, 5169–5177.
(7) Hou J.; Schacht J.; Giesselmann F.; Zugenmaier P. *Liq. Cryst.* **1997**, *22*, 409–417.
(8) Fafara A.; Wrobel S.; Haase W.; Marzec M.; Dabrowski R. *SPIE* **2002**, *4759*, 151–154.
(9) Philip J.; Lalanne J.; Marcerou J.; Sigaud G. *J. Phys., Paris II* **1994**, *4*, 2149–2159.
(10) Conradi M.; Musevic I.; Cepic M. *Phys. Rev. E* **2002**, *65*, 061705.
(11) Kimura Y.; Isono H.; Hayakawa R. *Eur. Phys. J. E* **2002**, *9*, 3–13.
(12) Fajar A.; Murai H.; Orihara H. *Phys. Rev. E* **2002**, *65*, 041704.
(13) Ortega J.; Folcia C.L.; Etxebarria J.; Ros M.B. *Liq. Cryst.* **2003**, *30*, 109–115.
(14) Liu Z.Q.; McCoy B.K.; Wang S.T.; Pindak R.; Caliebe W.; Barois P.; Fernandes P.; Nguyen H.T.; Hsu C.S.; Wang S.; et al. *Phys. Rev. Lett.* **2007**, *99*, 077802.
(15) Bourny V.; Fajar A.; Orihara H. *Phys. Rev. E* **2000**, *62*, R5903–R5906.
(16) Vaupotic N.; Cepic M.; Zeks B. *Ferroelectrics* **2000**, *245*, 175–184.
(17) Douali R.; Legrand C.; Laux V.; Isaert N.; Joly G.; Nguyen H.T. *Phys. Rev. E* **2004**, *69*, 031709.
(18) Pandey M.B.; Dhar R.; Agrawal V.K.; Dabrowski R.; Tykarska M. *Liq. Cryst.* **2004**, *31*, 973–987.
(19) Pandey M.B.; Dhar R.; Agrawal V.K.; Khare R.P.; Dabrowski R. *Phase Transitions* **2003**, *76*, 945–958; Pandey M.B.; Dhar R.; Dabrowski R. *Phil. Mag.* **2008**, *88*, 101–119.
(20) Hill N.E.; Vaughan W.E.; Price A.H.; Davies M. *Dielectric Properties and Molecular Behaviour*; pp. 1–106; Van Nostrand Reinhold: London, 1969.
(21) Srivastava S.L.; Dhar R. *Ind. J. Pure Appl. Phys.* **1991**, *29*, 745–751.
(22) Gouda F.M.; Skarp K.; Lagerwall S.T. *Ferroelectrics* **1991**, *113*, 165–206.
(23) Srivastava S.L. *Proc. Natn. Acad. Sci. India* **1993**, *63*, 311–332; Dhar R. *Ind. J. Pure Appl. Phys.* **2004**, *42*, 56–61.
(24) Pandey M.B.; Dhar R.; Agrawal V.K.; Dabrowski R. *Phase Transitions* **2005**, *78*, 457–470; Pandey M.B.; Dhar R.; Dabrowski R. *Ferroelectrics* **2006**, *343*, 83–100.
(25) Pandey M.B.; Dabrowski R.; Dhar R. *Physica B* **2007**, *387*, 25–31.
(26) Carlsson T.; Zeks B.; Filipic C.; Levstik A. *Phys. Rev. A* **1990**, *42*, 877–889.
(27) Skarabot M.; Kocevar K.; Blinc R.; Heppke G.; Musevic I. *Phys. Rev. E* **1999**, *59*, R1323–R1326.
(28) Pandey M.B.; Dhar R.; Dabrowski R. *J. Phys. Condensed Matter* **2008**, *20*, 115207.
(29) Skarabot M.; Cepic M.; Zeks B.; Blinc R.; Heppke G.; Kityk A.V.; Musevic I. *Phys. Rev. E* **1998**, *58*, 575–584.